Proceedings of 2016 International Automatic Control Conference (CACS)
The Evergreen Laurel Hotel, Taichung, Taiwan, November 09-11, 2016

# An Improved Inverse Kinematics Solution of 6R-DOF Robot Manipulators with Euclidean Wrist Using Dual Quaternions

Leoro Josuet, Betancourt Carlos, Lin Hsien-I, Hsiao Te-Sheng, Wang Chun-Sheng

***Abstract*—The present work focuses on the development of a methodology that can be used to solve the inverse kinematics of 6R robot manipulators with Euclidean wrist. Dual quaternions are used as screw motion operators to perform line transformations to the joint axes. The transformations are performed after each joint angle is found. This process accommodates the robot pose on each step from the initial pose to the final pose when all the joint angles have been found. In each step, the appropriate sub problems of Paden-Kahan are used to find the joint angles. The main contribution of the presented methodology is that it is a more general solution than previous approaches. Additionally, an extension of the second sub problem of Paden-Kahan is derived for parallel axes. The proposed algorithm can be used to solve the inverse kinematics problem of most of the 6R robot manipulator configurations, with or without shoulder offset, and with or without intersecting axes of the first and second joint.**

## I. Introduction

Kinematics studies the motion of bodies without considering the forces or moments that causes the motion. The kinematics of a robot manipulator is a fundamental problem in the robotics field [1]. There exist two kinematics problems, the forward kinematics problem and the inverse kinematics problem. The former focuses on finding the position and orientation of the end effector given the joints' angles. The latter focuses on finding the joints' angles given the position and orientation of the end effector. The inverse kinematics problem is a more complex process than the forward kinematics, and in general, the solving methods vary depending on the robot configuration.

The most common method to represent rigid transformations is based on the Denavit-Hartenberg notation and the homogeneous transformation matrices [1]. In this method the coordinate systems of each joint is described with respect to the previous one. Due to this representation some singularity problems may occur [2] [3]. Additionally, homogeneous transformation matrices are highly redundant to represent six independent degrees of freedom, since sixteen parameters are used to represent them. This redundancy can introduce numerical problems in calculations, wastes storage, and often increases the computational cost of algorithms [4].

The representation of rigid transformations by using screw theory has become one of the most important methods in the last few decades. A screw motion is represented as a linear motion along an axis with a rotation motion by an angle about the same axis in relation to the inertial frame [5]. In [3], homogenous transformation matrices and screw motion applied to robot kinematics are studied and compared in terms of singularity, computational efficiency and accuracy. In their work, they show screw theory based rigid transformations are more accurate and computed faster than homogeneous transformation matrices when applied to inverse kinematics. In addition, screw theory can avoid singularity because the coordinates of the joint axes and the end effector are transformed with respect to the base coordinate.

In [2] an inverse kinematics algorithm for 6R-DOF robot manipulator was developed using screw theory and exponential mapping as rigid body transformation operators. In their work they present an approach to solve the inverse kinematics of a specific robot configuration, where the axes of the first joint and the second joint do not intersect. This made the application of the known Paden-Kahan sub problems on the robot unsuitable. In their proposed solution, the first, second and third joint angles are solved by using the solution of a new sub-problem for three non-intersecting axes. For this sub-problem, two of the axes are parallel and non-coplanar to the third. Therefore, this algorithm can only be used for specific configurations where this requirement is present.

Dual quaternions can be used as rigid transformation operators to express screw motion. In fact, the dual quaternion is the most compact and efficient dual operator to express spatial transformations [6] [7] [8]. In addition, quaternions offer a more intuitive framework for using and understanding the effects of three-dimensional rotations because the axis and angle of rotation appear explicitly in their definition [6]. Besides, eight parameters are used to represent a rigid body transformation in contrast with the sixteen parameters used by homogeneous transformation matrices.

Sariyildiz and Temeltas presented a method to solve the inverse kinematics of a 6R serial robot manipulator using dual quaternions as rigid transformation operators and Plücker coordinates for line transformation [3]. In their work, the

Leoro Josuet is a PhD student in Electrical Engineering and Computer Science, National Chiao Tung University, Hsinchu, Taiwan 30010, R.O.C. (email: jl2005ec@gmail.com).

Betancourt Carlos is a PhD student in Electrical and Mechanical Engineering, National Taipei University of Technology, Taipei, Taiwan 10608, R.O.C. (email:carlos.betancourt.b@gmail.com).

Lin Hsien-I is with the Graduate Institute of Automation Technology, National Taipei University, Taipei, Taiwan 10608, R.O.C. (e-mail: sofin@ntut.edu.tw).

Hsiao Te-Sheng is with the Electrical and Computer Engineering Department, National Chiao Tung University, Hsinchu, Taiwan 30010, R.O.C. (corresponding author to provide phone: +88635131249; e-mail: tshsiao@cn.nctu.edu.tw).

Wang Chun-Sheng is with the Industrial Technology Research Institute, Mechanical and Mechatronics Systems Research Labs, Hsinchu, Taiwan 31040, R.O.C. (e-mail: arsheng1209@itri.org.tw).

inverse kinematics problem is also solved by dividing it into Paden-Kahan sub problems. In [9], their method was improved and compared against other methods that use exponential mapping operators and quaternions operators in the screw theory framework. Their results show that the methods that use quaternion and dual quaternion as a screw motion operator are more computationally efficient than exponential mapping method. Furthermore, dual quaternion method performed better than quaternion method. However, their algorithm can only be applied for configurations where the axes of the first and second joint intersect, because of the use of sub-problem 2 to find their respective angles.

The present work presents an alternative procedure also based on Plücker coordinates for line transformation and dual quaternions operators for rigid body transformations, but with the advantage that it can be applied to 6R-DOF robot configurations with or without shoulder offset, and without the condition of intersection of the axes of the first and second joints. This approach is suitable for the majority of configurations of 6R robot manipulators with Euclidean wrist.

The paper is divided as follows. In Section II, a mathematical background for quaternions, dual quaternions, dual quaternion screw operators and Plücker coordinates is provided. In Section III, an extension of the Paden-Kahan sub-problem 2 for parallel axes is presented. In Section IV, the proposed procedure to solve the inverse kinematics is explained step by step. In Section V, some simulation results are shown.

## II. Mathematical Background

This section provides a brief introduction to quaternions, dual quaternions, Plücker coordinates and the use of dual quaternions as rigid body transformation operators using screw theory. The definitions provided here are the necessary to understand the proposed algorithm for solving the inverse kinematics of robot manipulators. For a more detailed introduction of quaternions refer to [10] [11] [12], dual quaternions refer to [7][13][14] and for a description of the screw theory and derivation of the dual quaternion operators to represent screw motions refer to [15][16][17]. The notation used for quaternions and dual quaternions operations is the same as used in [3].

### A. Quaternions

Quaternions are an extension of complex numbers to formulate a four dimensional manifold.

$$\boldsymbol{q} = s + x\boldsymbol{i} + y\boldsymbol{j} + z\boldsymbol{k} \tag{1}$$

where s, x, y and z are the numerical values, while i, j and k are the imaginary components. The imaginary components follow the next properties:

$$\boldsymbol{i}^2 = \boldsymbol{j}^2 = \boldsymbol{k}^2 = -1 \tag{2}$$

And

$$\begin{array}{ll} \boldsymbol{ij} = \boldsymbol{k} & \boldsymbol{ji} = -\boldsymbol{k} \\ \boldsymbol{jk} = \boldsymbol{k} & \boldsymbol{kj} = -\boldsymbol{i} \\ \boldsymbol{ki} = \boldsymbol{k} & \boldsymbol{ik} = -\boldsymbol{j} \end{array}$$

It is more common to represent quaternions as two components, the vector component $\boldsymbol{v} = (x\boldsymbol{i} + y\boldsymbol{j} + z\boldsymbol{k})$ and the scalar component as shown in (3).

$$\boldsymbol{q} = (s,\ \boldsymbol{v}) \tag{3}$$

The arithmetic operations relevant for this paper are shown next:

Addition

$$\boldsymbol{q}_1 + \boldsymbol{q}_2 = (s_1 + s_2,\ \boldsymbol{v}_1 + \boldsymbol{v}_2) \tag{4}$$

Multiplication

$$\boldsymbol{q}_1 \otimes \boldsymbol{q}_2 = (s_1 s_2 - \boldsymbol{v}_1 \cdot \boldsymbol{v}_2,\ s_1\boldsymbol{v}_2 + s_2\boldsymbol{v}_1 + \boldsymbol{v}_1 \times \boldsymbol{v}_2) \tag{5}$$

Conjugate

$$\boldsymbol{q}^* = (s,\ -\boldsymbol{v}) \tag{6}$$

Magnitude

$$\|\boldsymbol{q}\|^2 = \boldsymbol{q} \otimes \boldsymbol{q}^* \tag{7}$$

Inverse

$$\boldsymbol{q}^{-1} = \boldsymbol{q}^* / \|\boldsymbol{q}\|^2 \tag{8}$$

For a unit quaternion, the magnitude $\|\boldsymbol{q}\|^2 = 1$, and therefore the inverse $\boldsymbol{q}^{-1} = \boldsymbol{q}^*$. A unit quaternion can be used to represent a rotation of an angle $\theta$ about a unit axis $\boldsymbol{n}$ in three-dimensional space:

$$\boldsymbol{q}_r = (cos(\theta/2),\ \boldsymbol{n}sin(\theta/2)) \tag{9}$$

A point can be represented by a quaternion with the scalar part equal to zero. Let $\boldsymbol{p} = p_x\boldsymbol{i} + p_y\boldsymbol{j} + p_z\boldsymbol{k}$ be a point in three-dimensional space, its quaternion representation is given by:

$$\boldsymbol{q}_p = (0,\ p_x\boldsymbol{i} + p_y\boldsymbol{j} + p_z\boldsymbol{k}) \tag{10}$$

The rotation of $\boldsymbol{p}$ using the rotation quaternion given in (9) is defined as:

$$\boldsymbol{q}_{pr} = \boldsymbol{q}_r \otimes \boldsymbol{q}_p \otimes \boldsymbol{q}_r^* \tag{11}$$

### B. Dual Quaternions

When quaternions are combined with dual number theory, the dual quaternions are obtained. A dual quaternion can be defined as:

$$\widehat{\boldsymbol{q}} = \boldsymbol{q} + \epsilon\boldsymbol{q}^0 \tag{12}$$

where both $\boldsymbol{q}$ and $\boldsymbol{q}^0$ are quaternions, $\boldsymbol{q}$ is the real part and $\boldsymbol{q}^0$ is the dual part. Combining the algebra operations associated with quaternions with the additional dual factor $\epsilon$, the dual quaternion arithmetic is formed. The arithmetic operations of dual quaternions relevant to this paper are shown next:

Addition

$$\widehat{\boldsymbol{q}}_1 + \widehat{\boldsymbol{q}}_2 = (\boldsymbol{q}_1 + \boldsymbol{q}_2) + \epsilon(\boldsymbol{q}_1^0 + \boldsymbol{q}_2^0) \tag{13}$$

Multiplication

$$\widehat{\boldsymbol{q}}_1 \odot \widehat{\boldsymbol{q}}_2 = (\boldsymbol{q}_1 \otimes \boldsymbol{q}_2) + \epsilon(\boldsymbol{q}_1 \otimes \boldsymbol{q}_2^0 + \boldsymbol{q}_2 \otimes \boldsymbol{q}_1^0) \tag{14}$$

Conjugate

$$\widehat{\boldsymbol{q}}^* = \boldsymbol{q}^* + \epsilon(\boldsymbol{q}^0)^* \tag{15}$$

Magnitude

$$\| \widehat{\boldsymbol{q}} \|^2 = \widehat{\boldsymbol{q}} \odot \widehat{\boldsymbol{q}}^* \tag{16}$$

Inverse

$$\widehat{\boldsymbol{q}}^{-1} = \widehat{\boldsymbol{q}}^* / \| \widehat{\boldsymbol{q}} \|^2 \tag{17}$$

where "$\otimes$" and "$\odot$" denote quaternion and dual quaternion product, respectively. Similarly to quaternions, for a unit dual quaternion we have $\| \widehat{\boldsymbol{q}} \|^2 = 1$, and the inverse $\widehat{\boldsymbol{q}}^{-1} = \widehat{\boldsymbol{q}}^*$.

### C. Plücker Coordinates

A line $\boldsymbol{L}(\boldsymbol{p}, \boldsymbol{d})$ in space is completely defined by two vectors, a point $\boldsymbol{p}$ that indicates the position of an arbitrary point on $\boldsymbol{L}$, and a free direction vector that defines the direction of the line $\boldsymbol{L}$. Each point on the line is given a parameter value that satisfies (18).

$$\boldsymbol{x} = \boldsymbol{p} + t\boldsymbol{d} \tag{18}$$

Plüucker coordinates is an alternative representation that uses two free vectors. A line in Plücker coordinates is denoted by $\boldsymbol{L}_{pl}(\boldsymbol{d}, \boldsymbol{m})$. Both $\boldsymbol{d}$ and $\boldsymbol{m}$ are free vectors. The vector $\boldsymbol{d}$ represents the direction of the line $\boldsymbol{L}_{pl}$, while $\boldsymbol{m}$ is the moment of $\boldsymbol{d}$ about the chosen reference origin and is calculated by using (19). Note that $\boldsymbol{m}$ is independent of which point $\boldsymbol{p}$ on the line is chosen because it satisfies (20). The advantages of the Plücker coordinates is that they are homogeneous: $\boldsymbol{L}_{pl}(k\boldsymbol{d}, k\boldsymbol{m})$, $k \in \mathbb{R}$, represents the same line, while $\boldsymbol{L}(k\boldsymbol{p}, k\boldsymbol{d})$ does not [12].

$$\boldsymbol{m} = \boldsymbol{p} + \times \boldsymbol{d} \tag{19}$$

$$\boldsymbol{p} \times \boldsymbol{d} = (\boldsymbol{p} + t\boldsymbol{d}) \times \boldsymbol{d} \tag{20}$$

Plücker coordinates can also be used to find the point of intersection of two lines. Let $\boldsymbol{L}_1 = (\boldsymbol{m}_1, \boldsymbol{d}_1)$ and $\boldsymbol{L}_2 = (\boldsymbol{m}_2, \boldsymbol{d}_2)$ be two non-parallel and coplanar lines in Plücker coordinates. The point of intersection $\boldsymbol{P}_{int}$ of the lines $\boldsymbol{L}_1$ and $\boldsymbol{L}_2$ can be found by using (21) or (22).

$$\boldsymbol{p}_{int} = \boldsymbol{d}_1 \times \boldsymbol{m}_1 + (\boldsymbol{d}_2 \times \boldsymbol{m}_2 \cdot \boldsymbol{d}_1)\boldsymbol{d}_1 \tag{21}$$

$$\boldsymbol{p}_{int} = \boldsymbol{d}_2 \times \boldsymbol{m}_2 + (\boldsymbol{d}_1 \times \boldsymbol{m}_1 \cdot \boldsymbol{d}_2)\boldsymbol{d}_2 \tag{22}$$

Finally, a line in Plücker coordinates can be represented using a dual quaternion by using the definition:

$$\widehat{\boldsymbol{L}} = (0, \boldsymbol{d}) + \epsilon(0, \boldsymbol{m}) \tag{23}$$

### D. Dual Quaternion as rigid body transformation operator

A screw motion is defined by a rotation about a line and a translation along the same line. Chasles' theorem states that all rigid body motions in three-dimensional space are equivalent to a screw motion [17]. The representation of a screw motion using a dual quaternion is defined as:

$$\widehat{\boldsymbol{q}} = cos(\widehat{\boldsymbol{\theta}}/2) + sin(\widehat{\boldsymbol{\theta}}/2)\widehat{\boldsymbol{d}} \tag{24}$$

where $\widehat{\boldsymbol{\theta}} = \theta + \epsilon k$, $\widehat{\boldsymbol{d}} = \boldsymbol{d} + \epsilon \boldsymbol{m}$, is the rotation angle, $k$ is the screw's pitch, and $\boldsymbol{d}$ and $\boldsymbol{m}$ are the direction and moment of the line about which the screw motion is applied. For a revolute joint $k = 0$, then (24) can be rewritten as:

$$\widehat{\boldsymbol{q}} = (cos(\theta/2),\ sin(\theta/2)\boldsymbol{d})\ +\ \epsilon(0,\ sin(\theta/2)\boldsymbol{m}) \tag{25}$$

A line in dual quaternion form $\widehat{\boldsymbol{L}}$ can be transformed to $\widehat{\boldsymbol{L}}_R$ by using the transformation operator from (25) as follows.

$$\widehat{\boldsymbol{L}}_R = \widehat{\boldsymbol{q}} \odot \widehat{\boldsymbol{L}} \odot \widehat{\boldsymbol{q}}^* \tag{26}$$

Multiple transformations operators can be combined by using (27). Then (26) can be used to apply multiple rigid body transformations to $\widehat{\boldsymbol{L}}$.

$$\widehat{\boldsymbol{Q}} = \widehat{\boldsymbol{q}}_1 \odot \widehat{\boldsymbol{q}}_2 \odot ... \odot \widehat{\boldsymbol{q}}_n \tag{27}$$

## III. Paden-Kahan Sub-problem 2 Extension for Parallel Axes

The method to solve the inverse kinematics problem based on screw theory generally reduces the full inverse kinematics into appropriate sub-problems whose solutions are known [18]. Among these sub-problems the most widely used are the three Paden-Kahan sub-problems: rotation about a single axis, rotation about two subsequent axes, and rotation to a given distance. Named sub-problems 1, 2 and 3, respectively. Their definitions can be found in [17].

To use sub-problem 2, a necessary condition is that the two axes must intersect. Tan and Xiao in [18] proposed an extension of this sub-problem that solve the rotation about two subsequent axes that do not intersect. Nevertheless, this extension is not applicable if the axes are parallel. For two parallel axes, usually the planar RR robot solution is used, since it is already well-defined. In our approach, the second and third joint angles are found using the position of the wrist, as it will be explained later, which makes the use of the planar RR solution appropriate. However, there are two disadvantages of using the RR solution in our procedure, especially for robot configurations with shoulder offset. First, it would be necessary to project the wrist position to a plane where the second and third joints are located after rotating the first joint. And second, for shoulder left and shoulder right solutions, correction in the joint angles of the second and third joints must be done since the direction of their respective axes changes.

As an alternative solution, an extension of sub-problem 2 for parallel axes that is compact and takes into account these two disadvantages is proposed. Thus making this solution useful to solve more general robot configurations. The new extension of sub-problem 2 corresponds to a rotation of a point $\boldsymbol{p}$ about the axis of $\xi_1$ by $\theta_1$ and then about the axis of $\xi_2$ by $\theta_2$, so that the final location of $\boldsymbol{p}$ is coincident with the point $\boldsymbol{q}$. This motion is illustrated in Fig. 1. The points $\boldsymbol{r}_1$ and $\boldsymbol{r}_2^{'}$ are any points on the axes $\xi_1$ and $\xi_2$, respectively, and $\xi_1$ and $\xi_2$ are parallel.

To solve this problem, first define the unit vector $\boldsymbol{\omega_1}$ on the same directions of the axes $\xi_1$ and $\xi_2$. Then, by using $\boldsymbol{r}_1$ and $\boldsymbol{r}_2^{'}$ find a point $\boldsymbol{r}_2$:

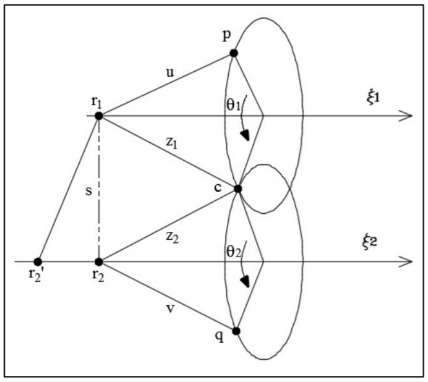


Fig. 1. Sub-problem 2 extension for parallel axes.

$$\boldsymbol{r} = \boldsymbol{r}_1 - \boldsymbol{r}_2^{'}$$
$$\boldsymbol{r}_{\boldsymbol{\omega_1}} = (\boldsymbol{r} \cdot \boldsymbol{\omega_1})\boldsymbol{\omega_1}$$
$$\boldsymbol{r}_2 = \boldsymbol{r}_2^{'} - \boldsymbol{r}_{\boldsymbol{\omega_1}}$$

Note that the segment $\boldsymbol{r}_1\boldsymbol{r}_2$ is perpendicular to the axes $\xi_1$ and $\xi_2$. Let us define the vector $\boldsymbol{s} = \boldsymbol{r}_1 - \boldsymbol{r}_2$ and the unit vector $\boldsymbol{\omega_2}$ on the direction of $\boldsymbol{s}$. Let us also define the vectors: $\boldsymbol{u} = \boldsymbol{p} - \boldsymbol{r}_1$, $\boldsymbol{v} = \boldsymbol{q} - \boldsymbol{r}_2$, $\boldsymbol{z}_1 = \boldsymbol{c} - \boldsymbol{r}_1$, $\boldsymbol{z}_2 = \boldsymbol{c} - \boldsymbol{r}_2$. Note that:

$$\|\boldsymbol{u}\| = \|\boldsymbol{z_1}\| \tag{28}$$
$$\|\boldsymbol{v}\| = \|\boldsymbol{z_2}\| \tag{29}$$

Observe that if the vectors $\boldsymbol{z}_1$ and $\boldsymbol{z}_2$ are found, the position of point $\boldsymbol{c}$ can easily be computed using the definition of this vectors ($\boldsymbol{c} = \boldsymbol{z}_1 + \boldsymbol{r}_1$ or $\boldsymbol{c} = \boldsymbol{z}_2 + \boldsymbol{r}_2$), and the problem is reduced into two sub-problems 1. The rotation of the point $\boldsymbol{p}$ around $\xi_1$ to the point $\boldsymbol{c}$, and from this position around $\xi_2$ to the point $\boldsymbol{q}$.

Let us define also the vector $\boldsymbol{z}_2$:

$$\boldsymbol{z_2} = \alpha\boldsymbol{\omega_1} + \beta\boldsymbol{\omega_2} + \gamma\boldsymbol{\omega_3} \tag{30}$$

where: $\boldsymbol{\omega_3} = \boldsymbol{\omega_1} \times \boldsymbol{\omega_2}$

Observe that this can be done because the set of vectors $\boldsymbol{\omega_1}$, $\boldsymbol{\omega_2}$ and $\boldsymbol{\omega_3}$ is an orthonormal basis. The expressions $\alpha$, $\beta$ and $\gamma$ are constants that have to be found. To find $\alpha$ take the projection of vectors $\boldsymbol{u}$ or $\boldsymbol{v}$ over $\boldsymbol{\omega_1}$:

$$\alpha = \boldsymbol{\omega_1} \cdot \boldsymbol{u} = \boldsymbol{\omega_2} \cdot \boldsymbol{v}$$

The constant $\beta$ is also defined as a dot product:

$$\beta = \boldsymbol{z_2} \cdot \boldsymbol{\omega_2} \tag{31}$$

To find the value of $\beta$, use the cosine theorem on the triangle $\boldsymbol{r_1 r_2 c}$:

$$\|\boldsymbol{z}_1\|^2 = \|\boldsymbol{z}_2\|^2 + \|\boldsymbol{s}\|^2 - 2\|\boldsymbol{z}_2\|\|\boldsymbol{s}\|cos(\theta) \tag{32}$$

Note that:

$$\|\boldsymbol{z}_2\|\|\boldsymbol{s}\|cos(\theta) = \boldsymbol{z}_2 \cdot \boldsymbol{s} \tag{33}$$

And also:

$$\boldsymbol{s} = \|\boldsymbol{s}\|\boldsymbol{\omega_2} \tag{34}$$

Replacing (28), (29), (31), (33) and (34) in (32) we get:

$$\|\boldsymbol{u}\|^2 = \|\boldsymbol{v}\|^2 + \|\boldsymbol{s}\|^2 - 2\|\boldsymbol{s}\|\beta \tag{35}$$

And finally, $\beta$ can be computed by:

$$\beta = \frac{\|\boldsymbol{p}\|^2 - \|\boldsymbol{q}\|^2 - \|\boldsymbol{s}\|^2}{-2\|\boldsymbol{s}\|} \tag{36}$$

To compute $\gamma$ use the norm of the vector $\boldsymbol{z}_2$:

$$\|\boldsymbol{z}_2\|^2 = \|\boldsymbol{v}\|^2 = \alpha^2 + \beta^2 + \gamma^2 \tag{37}$$

From this, $\gamma$ can computed as:

$$\gamma = \pm\sqrt{\|\boldsymbol{v}\|^2 - \alpha^2 - \beta^2} \tag{38}$$

By substituting $\alpha$, $\beta$ and $\gamma$ into (30), $\boldsymbol{z}_2$ can be found, and hence $\boldsymbol{c}$.

Then the two sub-problem 1 explained before can be used to find $\theta_1$ and $\theta_2$. If there are multiple solutions of $\boldsymbol{c}$, each of these solutions gives a value for $\theta_1$ and $\theta_2$. Two solutions exist in the case where the circles in Fig. 1 intersect at two points, one solution when the circles are tangential, and none when the circles do no not intersect.

## IV. 6R-DOF Robot Inverse Kinematics

To explain the proposed procedure for solving the inverse kinematics of a 6R-DOF robot manipulator, the Stäubli RX160 is used as an example. A schematic of the robot is shown in Fig. 2. In this robot's configuration the first and second joints' axes do not intersect. This configuration is common in a variety of robot manipulators. However, the application of the known Paden-Kahan sub problems to solve the full inverse kinematic problem is unsuitable for this particular configuration [2]. The procedure explained in this work can be used to solve the inverse kinematics of this configuration and other common configurations where the first and second joints' axes intersect.

Before starting the procedure, the axes for all joints must be determined. First, draw each joint z-axis with its direction and label them from one to six, one being the axis of the first joint and six the axis of the last joint. Then a point laying in the line of each axis must be selected. The location of this point can be chosen as desired. However, an exception is applied if the first and second axis do not intersect, or if the configuration has a shoulder offset. If one of these conditions is present, the points for the second and third axes must be selected in such a way that they do not lay in the line of action of the first joint axis. Preferably, select a point that is located in the link that joins the two joints. Also, for the fifth joint select the point of intersection of the fourth and fifth axes (position of the wrist). For the example given here, using the base coordinate frame as reference, the next directions are determined:

$$\begin{array}{lll} \boldsymbol{d}_1 = [0;0;1] & \boldsymbol{d}_2 = [0;1;0] & \boldsymbol{d}_3 = [0;1;0] \\ \boldsymbol{d}_4 = [0;0;1] & \boldsymbol{d}_5 = [0;1;0] & \boldsymbol{d}_6 = [0;0;1] \end{array} \tag{39}$$

And the chosen points are:

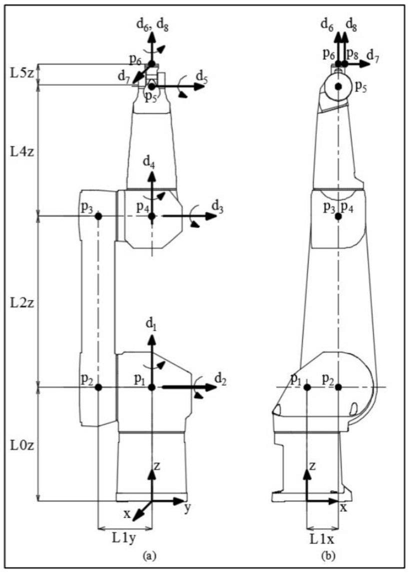


Fig. 2. Stäubli RX160 schematic, (a) front view, (b) right view.

$$\begin{aligned}
&\boldsymbol{p}_1 = [0;0;L0z] \quad \boldsymbol{p}_2 = [L1x;-L1y;L0z] \\
&\boldsymbol{p}_3 = [L1x;-L1y;L0z+L2z] \\
&\boldsymbol{p}_4 = [L1x;0;L0z+L2z] \\
&\boldsymbol{p}_5 = [L1x;0;L0z+L2z+L4z] \\
&\boldsymbol{p}_6 = [L1x;0;L0z+L2z+L4z+L5z]
\end{aligned} \tag{40}$$

Two additional axes are necessary to solve the joint angle of the sixth joint as it will be explained later. The seventh axis must point in the normal direction of the tool initial orientation, and the point $\boldsymbol{p}_7$ must be the same as $\boldsymbol{p}_6$. The eighth axis must have the same direction as the sixth axis, i.e. the tool approaching direction, and the point $\boldsymbol{p}_8$ must be in the line of the seventh axis with a small offset from $\boldsymbol{p}_6$. For the present example we have:

$$\boldsymbol{d}_7 = [1;0;0] \qquad \boldsymbol{d}_8 = \boldsymbol{d}_6 \tag{41}$$

$$\boldsymbol{p}_7 = \boldsymbol{p}_6 \qquad p_8 = \boldsymbol{p}_6 + 5 \times \boldsymbol{d}_7 \tag{42}$$

Then the moments $\boldsymbol{m}_i$ of each axis are calculated by using (19). Next, represent the lines $\widehat{\boldsymbol{L}}_2$, $\widehat{\boldsymbol{L}}_4$, $\widehat{\boldsymbol{L}}_5$, $\widehat{\boldsymbol{L}}_6$, and $\widehat{\boldsymbol{L}}_8$, corresponding to the axes 2, 4, 5, 6, 7 and 8, in dual quaternion form by using (23). It is important to remark that it is not necessary that the robot is positioned in its home position. In fact, positioning the robot extended vertically can ease the process.

For the rest of this paper, the joint angles will be named as $\theta_1$, $\theta_2$, $\theta_3$, $\theta_4$, $\theta_5$ and $\theta_6$, respectively. The desired position of the end effector is labeled as $\boldsymbol{Pe}_d$ and each of the desired orientation vectors are labeled $\boldsymbol{N}_d$ for the normal axis, $\boldsymbol{O}_d$ for the orientation axis and, $\boldsymbol{A}_d$ for the approaching axis. An additional initial step is to find the desired position of the robot wrist. The desired position of the wrist can be easily found for a Euclidean wrist. By using the end effector desired position, the desired approaching direction, and the length of link 5, the position of the wrist can be calculated by:

$$\boldsymbol{Pw}_d = \boldsymbol{Pe}_d - L5z * \boldsymbol{A}_d \tag{43}$$

The steps to solve the inverse kinematics of the robot manipulator shown in Fig. 2 are explained next.

Step 1: Find $\theta 1$ by using $\boldsymbol{Pw}_d$ and geometry. In this step the shoulder offset must be considered. Calculate $\theta 1$ by using (44), (45) and (46).

$$\alpha_1 = atan2(\boldsymbol{Pw}_d y, \boldsymbol{Pw}_d x) \tag{44}$$

$$\alpha_2 = atan2(b, \sqrt{\boldsymbol{Pw}_d x^2 + \boldsymbol{Pw}_d y^2 - b^2}) \tag{45}$$

$$\theta_1 = \alpha_1 \pm \alpha_2 + \pi \tag{46}$$

where $\boldsymbol{Pw}_d x$ and $\boldsymbol{Pw}_d y$ are the components of the projection of $\boldsymbol{Pw}_d$ onto a plane perpendicular to $\boldsymbol{d}_1$, and $b$ is the shoulder offset. It is important to note that the robot manipulator from Fig. 2 does not have a shoulder offset. However, we are presenting a general solution for other configurations were the shoulder offset may exist. Equation (46) gives two possible solutions for $\theta_1$, namely shoulder left and shoulder right. Once $\theta_1$ is obtained, represent the transformation operator $\widehat{\boldsymbol{q}}_1$ using (25).

Step 2: Find $\theta_2$ and $\theta_3$ by applying the proposed sub-problem 2 for parallel axes using $\boldsymbol{d}_2$, $\boldsymbol{d}_3$ and the position of the wrist. To find the required parameters for this sub-problem, first rotate $\boldsymbol{p}_2$, $\boldsymbol{p}_3$ and $\boldsymbol{p}_5$ using (9), (10) and (11) to obtain $\boldsymbol{p}_{2r1}$, $\boldsymbol{p}_{3r1}$ and $\boldsymbol{p}_{5r1}$. Rotate $\widehat{\boldsymbol{L}}_2$ using $\widehat{\boldsymbol{q}}_1$ and (26) to obtain $\widehat{\boldsymbol{L}}_{2r1}$; and from $\widehat{\boldsymbol{L}}_{2r1}$ obtain $\boldsymbol{d}_{2r1}$, where $\boldsymbol{p}_{2r1}$ means point 2 after rotating joint 1 an angle $\theta_1$ starting from the robot arm's reference position. The same meaning applies for $\boldsymbol{p}_{3r1}$, $\boldsymbol{p}_{5r1}$, $\widehat{\boldsymbol{L}}_{2r1}$ and $\boldsymbol{d}_{2r1}$. Then the parameters to use sub-problem 2 for parallel axes are $\boldsymbol{p} = \boldsymbol{p}_{5r1}$, $\boldsymbol{q} = \boldsymbol{Pw}_d$, $\boldsymbol{r}_1 = \boldsymbol{p}_{3r1}$, $\boldsymbol{r}_2 = \boldsymbol{p}_{3r1}$ and $\boldsymbol{d}_{2r1}$ being the direction of both $\xi_1$ and $\xi_2$. Here, again there are two solutions, namely elbow up and elbow down. Once $\theta_2$ and $\theta_3$ are obtained, again represent the transformation operators $\widehat{\boldsymbol{q}}_2$ and $\widehat{\boldsymbol{q}}_3$ using (25). Then combine the transformation operators using (27) to obtain $\widehat{\boldsymbol{Q}}_{123}$.

Step 3: Find $\theta_4$ and $\theta_5$ by applying sub-problem 2 using axes $\boldsymbol{d}_4$ and $\boldsymbol{d}_5$ and the position of the end effector. To find the required parameters for this sub-problem, first rotate $\widehat{\boldsymbol{L}}_4$ and $\widehat{\boldsymbol{L}}_7$ by using (26) and $\widehat{\boldsymbol{Q}}_{123}$ to obtain $\widehat{\boldsymbol{L}}_{4r123}$ and $\widehat{\boldsymbol{L}}_{7r123}$. The intersection of these two new lines gives as result the position of the end effector $\boldsymbol{Pe}_{r123}$. The intersection point can be found by using (21). Additionally, from $\widehat{\boldsymbol{L}}_{4r123}$ obtain $\boldsymbol{d}_{4r123}$. The direction $\boldsymbol{d}_{5r123} = \boldsymbol{d}_{2r1}$ since they are parallel, point into the same direction, and are not affected by the rotation of $\theta_2$ and $\theta_3$. Then the parameters to use sub-problem 2 are $\boldsymbol{p} = \boldsymbol{Pe}_{r123}$, $\boldsymbol{q} = \boldsymbol{Pe}_d$, $\boldsymbol{r} = \boldsymbol{Pw}_d$, the direction of the axis $\xi_1$ is $\boldsymbol{d}_{4r123}$ and the direction of $\xi_2$ is $\boldsymbol{d}_{5r123}$. Once $\theta_4$ and $\theta_5$ are obtained, again represent the transformation operators $\widehat{\boldsymbol{q}}_4$ and $\widehat{\boldsymbol{q}}_5$ using (25). And then combine the transformation operators using (27) to obtain $\widehat{\boldsymbol{Q}}_{12345}$.

Step 4: Find $\theta_6$ by applying sub-problem 1 and using $\boldsymbol{d}_6$ and two auxiliary points. To find the required parameters for this sub-problem, first rotate $\widehat{\boldsymbol{L}}_6$, $\widehat{\boldsymbol{L}}_7$ and $\widehat{\boldsymbol{L}}_8$ by using (26) and $\widehat{\boldsymbol{Q}}_{12345}$ to obtain $\widehat{\boldsymbol{L}}_{6r12345}$, $\widehat{\boldsymbol{L}}_{7r12345}$ and $\widehat{\boldsymbol{L}}_{8r12345}$. Furthermore, from $\widehat{\boldsymbol{L}}_{6r12345}$ obtain $\boldsymbol{d}_{6r12345}$. The first auxiliary point $\boldsymbol{p}_{aux1}$ is the intersection of $\widehat{\boldsymbol{L}}_{7r12345}$ and $\widehat{\boldsymbol{L}}_{8r12345}$. The second auxiliary point $\boldsymbol{p}_{aux2}$ is found by using (47).

$$\boldsymbol{p}_{aux2} = \boldsymbol{P}\boldsymbol{e}_d + 5 \times \boldsymbol{N}_d \tag{47}$$

Then the parameters to use sub-problem 1 are $\boldsymbol{p} = \boldsymbol{p}_{aux1}$, $\boldsymbol{q} = \boldsymbol{p}_{aux2}$, $\boldsymbol{r} = \boldsymbol{P}\boldsymbol{e}_d$ and the direction of the axis $\xi$ is $\boldsymbol{d}_{6r123}$. This concludes the procedure to solve the inverse kinematics.

## V. Simulation Results

The methodology explained in Section IV was programmed in MATLAB to solve the inverse kinematics of the Stubli RX160 robot manipulator. To verify that the proposed method can correctly solve the inverse kinematics, different tests were performed using groups of joints angles inside their range of movement. The forward kinematics were used to find the position and orientation of the end effector in each test. Next, the obtained vectors were used as the desired position and orientation for the inverse kinematics. Then, the proposed algorithm was applied to find the joint angles to compare them with the given ones. An example test is shown next, for the group of joint angles:

$$\theta_1 = 45^\circ \qquad \theta_2 = 30^\circ \qquad \theta_3 = -60^\circ$$
$$\theta_4 = 60^\circ \qquad \theta_5 = 15^\circ \qquad \theta_6 = 20^\circ$$

From the forward kinematics, the obtained end effector position, normal, orientation and approaching direction vectors are:

$$\boldsymbol{P}\boldsymbol{e}_d = [130.49384; 165.36244; 1904.87115]$$
$$\boldsymbol{N}_d = [0.49423; 0.85927; 0.13181]$$
$$\boldsymbol{O}_d = [0.76072; 0.50087; 0.41282]$$
$$\boldsymbol{A}_d = [0.42075; 0.10376; 0.90122]$$

The eight solutions obtained from the inverse kinematics are shown in Table I. In each test, all the obtained solutions were tested using the forward kinematics; and the same end effector position and orientation than the one given by the selected group of joint angles were obtained. The calculation time when eight solutions were obtained was in average 88 ms. This can be improved if additional constraints are given to reduce the number of solutions to calculate. The results obtained from the different tests performed validated the correctness of the method derived in this work.

TABLE I. Inverse kinematics solutions for an example test

| Sol No. | Joint | $\theta[^\circ]$ | Joint | $\theta[^\circ]$ |
|---|---|---|---|---|
| 1 | 1 | 44.999 | 4 | -14.669 |
| | 2 | -20.893 | 5 | -62.264 |
| | 3 | 60.000 | 6 | 86.078 |
| 2 | 1 | 44.999 | 4 | 165.330 |
| | 2 | -20.893 | 5 | 62.265 |
| | 3 | 60.000 | 6 | -93.922 |
| 3 | 1 | 44.999 | 4 | -120.000 |
| | 2 | 30.000 | 5 | -15.000 |
| | 3 | -60.000 | 6 | -160.000 |
| 4 | 1 | 44.999 | 4 | 60.000 |
| | 2 | 30.000 | 5 | -15.000 |
| | 3 | -60.000 | 6 | 20.000 |
| 5 | 1 | -135.000 | 4 | 130.857 |
| | 2 | -38.905 | 5 | -17.239 |
| | 3 | 49.800 | 6 | 126.968 |
| 6 | 1 | -135.000 | 4 | -49.142 |
| | 2 | -38.905 | 5 | 17.239 |
| | 3 | 49.800 | 6 | -53.032 |
| 7 | 1 | -135.000 | 4 | 166.124 |
| | 2 | 3.568 | 5 | -69.172 |
| | 3 | -49.800 | 6 | 84.152 |
| 8 | 1 | -135.000 | 4 | -13.876 |
| | 2 | 3.568 | 5 | 69.172 |
| | 3 | -49.800 | 6 | -95.848 |

## References

[1] M. W. Spong, S. Hutchinson, and M. Vidyasagar, *Robot modeling and control*. Wiley New York, 2006, vol. 3.
[2] Q. Chen, S. Zhu, and X. Zhang, "Improved inverse kinematics algorithm using screw theory for a six-dof robot manipulator," *International Journal of Advanced Robotic Systems*, vol. 12, 2015.
[3] E. Sariyildiz and H. Temeltas, "Solution of inverse kinematic problem for serial robot using dual quaterninons and plücker coordinates," in *2009 IEEE/ASME International Conference on Advanced Intelligent Mechatronics*. IEEE, 2009, pp. 338–343.
[4] S. Sahu, B. Biswal, and B. Subudhi, "A novel method for representing robot kinematics using quaternion theory," 2008.
[5] C. D. Crane III, J. Rico, and J. Duffy, "Screw theory and its application to spatial robot manipulators," *Center for Intelligent Machines and Robotics, University of Florida, Gainesville, FL, Technical Report*, 2009.
[6] J. Funda, R. H. Taylor, and R. P. Paul, "On homogeneous transforms, quaternions, and computational efficiency," *IEEE Transactions on Robotics and Automation*, vol. 6, no. 3, pp. 382–388, 1990.
[7] B. Kenwright, "Dual-quaternions: From classical mechanics to computer graphics and beyond, 1-11," *Source: www. xbdev. net*.
[8] L. Kavan, S. Collins, C. OSullivan, and J. Zara, "Dual quaternions for rigid transformation blending," *Trinity College Dublin, Tech. Rep. TCD-CS-2006-46*, 2006.
[9] E. Sariyildiz, E. Cakiray, and H. Temeltas, "A comparative study of three inverse kinematic methods of serial industrial robot manipulators in the screw theory framework," *International Journal of Advanced Robotic Systems*, vol. 8, no. 5, pp. 9–24, 2011.
[10] R. Mukundan, "Quaternions: From classical mechanics to computer graphics, and beyond," in *Proceedings of the 7th Asian Technology conference in Mathematics*, 2002, pp. 97–105.
[11] J. McDonald, "Teaching quaternions is not complex," in *Computer Graphics Forum*, vol. 29, no. 8. Wiley Online Library, 2010, pp. 2447–2455.
[12] H. Bruyninckx and J. Shutter, "Introduction to intelligent robotics," *Katholieke Universiteit de Leuven, Tech. Rep*, pp. 40–52, 2001.
[13] H.-L. Pham, V. Perdereau, B. V. Adorno, and P. Fraisse, "Position and orientation control of robot manipulators using dual quaternion feedback," in *IROS'10: International Conference on Intelligent Robots and Systems*. IEEE/RSJ, 2010, pp. 658–663.
[14] B. Kenwright, "A beginners guide to dual-quaternions," *WSCG'2012*, 2012.
[15] J.-H. Kim and V. R. Kumar, "Kinematics of robot manipulators via line transformations," *Journal of Robotic Systems*, vol. 7, no. 4, pp. 649–674, 1990.
[16] A. T. Yang and F. Freudenstein, "Application of dual-number quaternion algebra to the analysis of spatial mechanisms," *Journal of Applied Mechanics*, vol. 31, no. 2, pp. 300–308, 1964.
[17] R. M. Murray, Z. Li, S. S. Sastry, and S. S. Sastry, *A mathematical introduction to robotic manipulation*. CRC press, 1994.
[18] T. Yue-sheng and X. Ai-Ping, "Extension of the second paden-kahan sub-problem and its' application in the inverse kinematics of a manipulator," in *2008 IEEE Conference on Robotics, Automation and Mechatronics*. IEEE, 2008, pp. 379–381.